

# Experimental study of speed-dependent collisional effects of He and Ne on the 687.1 nm argon line

A. Bielski, S. Brym<sup>a</sup>, R. Ciuryło<sup>b</sup>, and J. Szudy

Institute of Physics, Nicholas Copernicus University, Grudziądzka 5/7, 87–100 Toruń, Poland

Received 5 November 1998 and Received in final form 9 July 1999

**Abstract.** Using a pressure-scanned Fabry-Perot interferometer precise measurements of the profiles of the 687.1 nm argon line perturbed by helium and neon pressures between 0.5 and 44 torr have been performed. Careful analysis of line shapes showed that for Ar–He the speed-dependent effects do not play any essential role. Contrary to that, for Ar–Ne these effects can give rise to noticeable decrease of the Doppler width determined using the Voigt profile. It was shown that for Ar–Ne the inclusion of speed-dependent effects can reduce the apparent dependence of the Doppler width on the neon density and cause the Doppler temperatures determined from the profiles to be consistent with the source temperature. The role of the Dicke narrowing is also discussed.

**PACS.** 32.70.-n Intensities and shapes of atomic spectral lines – 33.70.-w Intensities and shapes of molecular spectral lines and bands – 34.20.-b Interatomic and intermolecular potentials and forces, potential energy surfaces for collisions

## 1 Introduction

Shapes of collisionally broadened spectral lines at low pressures have long been analysed in terms of Voigt profiles, *i.e.* convolutions of Gaussian and Lorentzian distributions. The fundamental assumption made to derive the Voigt profile (VP) is that the collisional and Doppler line broadening are uncorrelated and the change of velocity during collisions can be neglected.

If the correlation between the collisional broadening and the velocity of the emitting atoms is taken into account, then as was shown by Berman [1] and Ward *et al.* [2] deviations from the Voigt profile may occur and give rise to an asymmetric line profile. Such correlation effects are included in the so-called speed-dependent Voigt profile (SDVP) [1,2].

Deviations from the Voigt profile may also be caused by velocity-changing collisions giving rise to the reduction of the Doppler width due to Dicke narrowing [3]. A more general treatment of the modification of the Doppler broadening by velocity-changing collisions was given in the framework of the so-called “soft-collision” model by Galatry [4] who treated the emitting atom as a particle in Brownian motion but neglected correlation between the emitter motion and the emitter-perturber collision. Two of us [5] used the soft-collision model to derive a speed-dependent Galatry profile (SDGP) in which both

speed-dependent effects and Dicke narrowing are included. In the two limiting cases the SDGP reduces either to the ordinary Galatry profile (GP) if the velocity-changing collisions are taken into account but correlation effects are omitted or the SDVP in opposite limit when correlation effects are included and Dicke narrowing is neglected. An alternative approach to this problem is the so-called “hard-collision” model [6,7] developed for the speed-dependent case by Lance *et al.* [8]. The unification of these two approaches in the speed-dependent case was proposed in references [9,10].

In recent years several laboratories have focused their attention on experimental studies of the influence of speed-dependent effects on the profiles of atomic and molecular lines [8,11–20]. Most of these studies deal with systems such that the mass  $m_P$  of the perturbing atom was much greater than the mass  $m_E$  of the emitter, *i.e.* the mass ratio  $\alpha = m_P/m_E$  was greater than 1. There are, however, indications that speed-dependent effects may also be important in cases when the perturber mass is close to or even less than that of the emitter. Since some aspects of statistical correlation between the collisions and the thermal motion as well as speed-dependence of line-shape parameters are still not well understood, further work is required in these areas.

This paper reports results of interferometric measurements of profiles of the 687.1 nm argon line perturbed by helium and neon. The pressure broadening and shift of this line was already studied in our laboratory in 1986 by Wawrzyński and Wolnikowski [21]. Since then our group

---

<sup>a</sup> *Present address:* Department of Physics, Pedagogical University, Żołnierska 14, 10–561 Olsztyn, Poland.

<sup>b</sup> e-mail: rciurylo@phys.uni.torun.pl

has developed the instrumental capability for very precise measurements of the emission line profiles. First of all, we have been able to increase the signal-to-noise ratio of our spectrometer to such a level that it enables one to obtain very accurate values of the line-shape parameters which are influenced by the correlations between the Doppler and collisional broadening as well as the speed-changing collisions.

We have therefore thought it useful to perform new measurements of the shape of the 687.1 nm Ar line perturbed by He and Ne in order to verify recent theoretical predictions that the speed-dependent narrowing of the Doppler component of an emission line may also be observed for systems with the mass ratio  $\alpha \leq 1$ . The 687.1 nm Ar line is suitable for experimental studies because it is strong enough and well isolated from neighbouring lines and, moreover, it has no hyperfine structure components which usually prevent evaluation of line shape parameters with the necessary accuracy.

In the present paper we report the results of such an experiment carried out at pressures of the perturbing gas (Ne or He) between 0.50 and 44 torr. In the experiment performed by Wawrzyński and Wolnikowski [21] the highest pressure was only 14 torr. In the present investigation the main attention was on the methods of numerical analysis of measured profiles, in particular those dealing with the evaluation of the Doppler temperature from the Doppler-Gaussian line width. In order to obtain reliable line-shape parameters a very careful analysis was carried out in order to take into account the instrumental contribution to the total Gaussian width.

## 2 Experimental

Experiments described in the present work were done using a spectrometer with a pressure-scanned Fabry-Perot interferometer (FPI) identical to that applied in our recent studies on the neon spectral lines [22]. The experimental set-up is similar to that used by Wawrzyński and Wolnikowski [21] but it has been modified in such a way that its precision is increased by about one order of magnitude in comparison to that of the previous version. A glow discharge tube of the type described in [23] was used as a light source. Light was collected from the positive column of the glow discharge (1.5 mA current) run at pressures in the range between 0.50 and 44 torr. Using a  $T$ -type (copper-constantan) thermocouple and procedures described by Ciuryło [24] the temperature of the emitting gas in the tube was determined to be close to 320 K. This value was used to determine the density numbers of perturbing gases at various pressures. It was found that the errors connected with the determination of the gas temperature of about 10–20 K cause the pressure broadening and shift rates to be subject to systematic errors between 3% and 6%.

Line profiles were recorded using a FPI [25] with dielectric coating and a 1.513 cm spacer (free spectral range  $330.5 \times 10^{-3} \text{ cm}^{-1}$ ). Following Jiglinskii and Kuchinskii [26], we have estimated the width  $\gamma_G$  (FWHM) of the

Gaussian component of the instrumental function of our FPI coming from the defects of the interferometer plates for the 687.1 nm line to be  $\gamma_G = 11 \times 10^{-3} \text{ cm}^{-1}$ . Measurements of the pressure shift of the line peak were made relative to the same line emitted from the electrodeless RF argon discharge tube, and maintained under constant conditions. The pressure of argon in the reference source was kept at 0.79 torr. The reference line was shifted about  $3 \times 10^{-3} \text{ cm}^{-1}$  from the line emitted from the glow discharge and this leads to a nonzero value of the shift when it is extrapolated to zero perturber density (see Figs. 2 and 7). The intensity distribution in a broadened line was registered using a photomultiplier in the photon counting mode.

All experiments described in the present work were performed on natural argon which is a mixture of three isotopes  $^{36}\text{Ar}$  (0.34%),  $^{38}\text{Ar}$  (0.06%) and  $^{40}\text{Ar}$  (99.60%). The contributions from the  $^{36}\text{Ar}$  and  $^{38}\text{Ar}$  isotopes were neglected so that the experimental interferograms were directly fitted to functions describing the response of the FPI to some theoretical profiles such as VP, SDVP, GP and SDGP. The fits were made using an algorithm given by Marquardt [27]. To analyse the quality of the fit we use the so-called weighted difference  $D_\sigma(\omega)$  defined by [22, 28]

$$D_\sigma(\omega) = \frac{O_{\text{exp}}(\omega) - O_{\text{fit}}(\omega)}{\sqrt{O_{\text{fit}}(\omega)}} \quad (1)$$

where  $O_{\text{exp}}(\omega)$  is the measured profile and  $O_{\text{fit}}(\omega)$  is the best fit value. In our case when the experimental profiles were monitored using a photomultiplier in the photon counting mode, the mean standard deviations corresponding to the best fit value at frequency  $\omega$  is equal to  $\sqrt{O_{\text{fit}}(\omega)}$ .

## 3 Voigt analysis

First, we have analysed the profiles of the 687.1 nm Ar line recorded by means of our FPI assuming that both the velocity-changing collisions and the Doppler-collision correlation can be neglected. In such a case the profile  $O_{\text{VP}}(\omega)$  registered by FPI can be written as a convolution of the Voigt profile and the instrumental function of FPI which has a form analogous to that first derived by Ballik [29]:

$$O_{\text{VP}}(\omega) = \frac{2}{\Omega} \left\{ \frac{1}{2} + \sum_{n=1}^{\infty} R^n e^{-nL} e^{-n^2(G^2+D^2)/4} \times \cos\left(\frac{2n\pi}{\Omega}(\omega - \omega_0 - \Delta)\right) \right\}. \quad (2)$$

Here  $\Omega$  is the free spectral range of FPI,  $\gamma_D = 2\omega_0\sqrt{2\ln 2}k_B T/(m_E c^2)$  and  $\gamma_L$  are the widths (FWHM) of the Doppler and Lorentzian component of the Voigt profile,  $\Delta$  is the pressure shift of the line with respect to unperturbed frequency  $\omega_0$  and  $R$  is the reflection coefficient of etalon mirrors. The reduced quantities

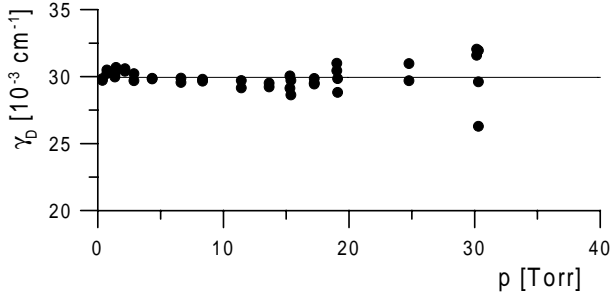


**Fig. 1.** Plots of the Doppler width  $\gamma_D$  (FWHM) of the 687.1 nm Ar line against the helium pressure  $p$  determined on the basis of the  $O_{VP}(\tilde{\nu})$  profile. The mean value of  $\gamma_D$  is marked by solid line (—).

$D = \pi\gamma_D/(\Omega\sqrt{\ln 2})$  and  $L = \pi\gamma_L/\Omega$  denote the reduced Doppler and Lorentzian widths, respectively.

It should be emphasized that, contrary to the original Ballik [29] formula, equation (2) takes into account the Gaussian component of the FPI instrumental function of the width  $\gamma_G$ . The reduced quantity  $G = \pi\gamma_G/(\Omega\sqrt{\ln 2})$  is thus the reduced Gaussian width of the instrumental function.

### 3.1 The 687.1 nm Ar line perturbed by He

In the case of perturbation by He, measurements were done at constant argon pressure 0.72 torr and the helium pressure was varied between 0.36 and 30 torr. The profiles recorded by our FPI were fitted to the profile  $O_{VP}(\omega)$ , equation (2), which represents a response of FPI to the ordinary Voigt profile. The values of the Doppler width  $\gamma_D$  determined from such fits are shown in Figure 1, where they are plotted against the helium pressure. It is seen that  $\gamma_D$  is independent of the pressure and the mean value  $\gamma_D = (29.95 \pm 0.94) \times 10^{-3} \text{ cm}^{-1}$  of the Doppler width corresponds to the Doppler temperature  $T_D = (331 \pm 20) \text{ K}$  which is very close to the gas temperature determined using the thermocouple.

The lack of the dependence of the Doppler width determined on basis of the ordinary Voigt profile on the helium pressure and the fact that the Doppler temperature found in this way is close to the gas temperature determined by means of a thermocouple, may be regarded as evidence that for the case of the 687.1 nm Ar line perturbed by He, velocity-changing collisions and correlation effects do not play any role.

The values of the Lorentzian width  $\gamma_L$  and the shift  $\Delta$  determined from the fits of our experimental profiles to the ordinary Voigt profile are shown in Figure 2 where they are plotted as functions of the number density  $N$  of helium. It is seen that both the width and shift are linear functions of  $N$  and can be approximated by the following relations:  $\gamma_L = \gamma_L^{(0)} + \beta N$ , and  $\Delta = \Delta^{(0)} + \delta N$ , where  $\beta$  and  $\delta$  denote the pressure broadening and shift coefficients, respectively. Here  $\gamma_L^{(0)}$  and  $\Delta^{(0)}$  are the residual Lorentzian width and shift corresponding to the zero density of perturbing gas. The nonzero value of  $\Delta^{(0)}$  is caused by the

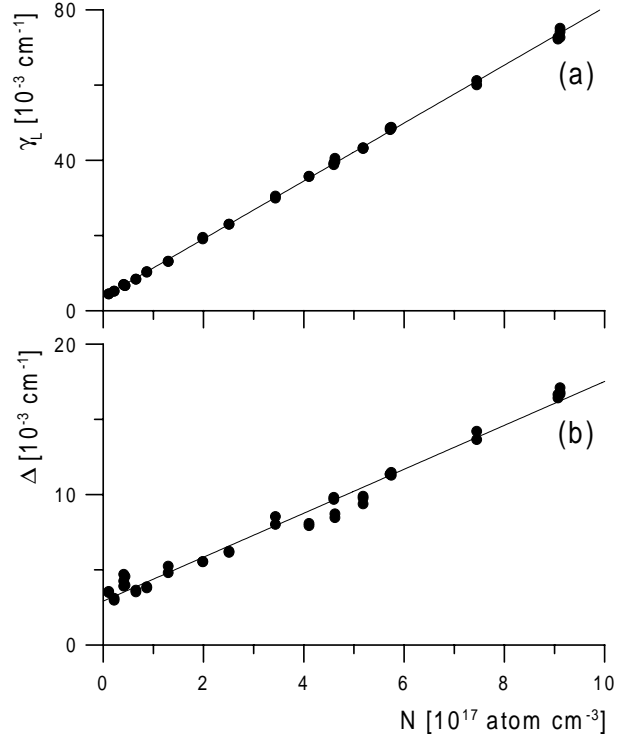


**Fig. 2.** Plots of (a) the Lorentzian width (FWHM)  $\gamma_L$  and (b) shift  $\Delta$  for the 687.1 nm Ar line against the helium density  $N$  determined on the basis of the  $O_{VP}(\tilde{\nu})$  profile. The fitted functions are plotted as solid lines (—).

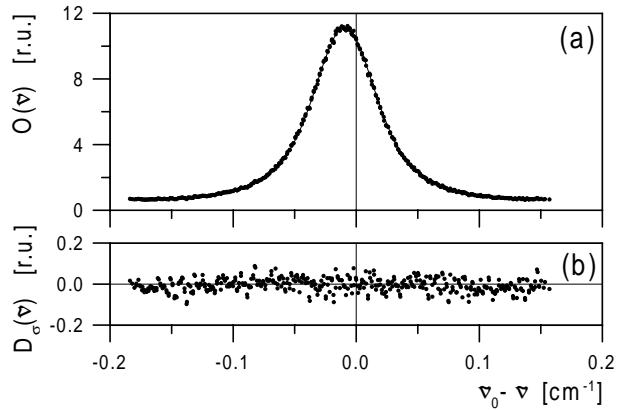


**Fig. 3.** (a) Shape of the 687.1 nm Ar line at helium pressure 17.23 torr, (●) experimental points, solid line (—) the best fit  $O_{VP}(\tilde{\nu})$  profile. (b) Weighted differences between the observed profile and the fitted  $O_{VP}(\tilde{\nu})$  profile.

fact the our shift measurements were performed in such a way that we have measured the position of the maximum of the spectral line emitted by the glow discharge source with respect to that of the same line emitted by reference source.

Figure 3a shows an example of the measured profile of the 687.1 nm Ar line recorded at 17.23 torr. The weighted differences  $D_\sigma(\omega)$  between the experimental and the best fit value obtained from the profile  $O_{VP}(\omega)$ , equation (2), are plotted in Figure 3b. It is seen that the profile

**Table 1.** Comparison of experimental values of the  $\beta$  and  $\delta$  coefficients (in units  $10^{-20} \text{ cm}^{-1}/\text{atom cm}^{-3}$ ) of the 687.1 nm argon line perturbed by helium with those calculated for different interatomic potentials. For experimental data the values of standard deviation are given.

Experimental	$\beta$	$\delta$	$\delta/\beta$
VP	$7.701 \pm 0.030$	$1.461 \pm 0.031$	$0.190 \pm 0.004$
Wawrzyński and Wolnikowski [21]	$8.94 \pm 0.11$	$1.53 \pm 0.08$	$0.17 \pm 0.01$
	$(7.83 \pm 0.10)$	$(1.34 \pm 0.07)$	
Theoretical	$\beta$	$\delta$	$\delta/\beta$
vdW	3.195	-1.160	-0.363
LJ	10.728	1.488	0.139

$O_{VP}(\omega)$  fits very well to the experimental data. Therefore we can conclude that under our conditions the shapes of the 687.1 nm Ar line perturbed by helium are very well described by the Voigt profile. This corroborates our conclusion that for the Ar–He system ( $\alpha = 0.1$ ) speed-dependent effects do not play any essential role.

Using the plots of the Lorentzian widths  $\gamma_L$  and shifts  $\Delta$  against the helium density the values of the pressure broadening  $\beta$  and shift  $\delta$  coefficients were determined from the slopes of straight lines plotted in Figure 2. These coefficients are listed in Table 1, where the values determined from the fits of experimental profiles to the profile  $O_{VP}(\omega)$ , equation (2), are denoted by “VP”. Table 1 also contains the experimental values determined by Wawrzyński and Wolnikowski [21]. It should be emphasized that the mean Doppler temperature determined in [21] for the same value of the discharge current in the Ar–He mixture and identical geometrical conditions was found to be  $(365 \pm 19)$  K which differs from the value  $(331 \pm 20)$  K determined in the present work. The cause of this discrepancy is that the line profile analysis in reference [21] was performed assuming the instrumental function to be that of the ideal FPI so that no instrumental contribution to the Gaussian width was included. Wawrzyński and Wolnikowski [21] have determined the values  $\beta$  and  $\delta$  of the pressure broadening and shift coefficient on the basis of the helium densities  $N$  which were determined from the measured pressure assuming the temperature of the Ar–He mixture to be equal to 365 K. These values of  $\beta$  and  $\delta$  are listed in the second row of Table 1. If we correct the Doppler temperature determined in [21] by the inclusion of the instrumental contribution to the Gaussian width then the Doppler temperature in the Ar–He mixture corresponding to the conditions in experiment by Wawrzyński and Wolnikowski [21] is found to be very close to 320 K, *i.e.* the gas temperature in the present study. The values of  $\beta$  and  $\delta$  given in parentheses in Table 1 are the experimental values of reference [21] recalculated for the temperature 320 K.

### 3.2 The 687.1 nm Ar line perturbed by Ne

In the case of perturbation by Ne-atoms, the measurements of the profiles of the 687.1 nm Ar line were carried out for neon pressures between 0.50 and 43.79 torr.

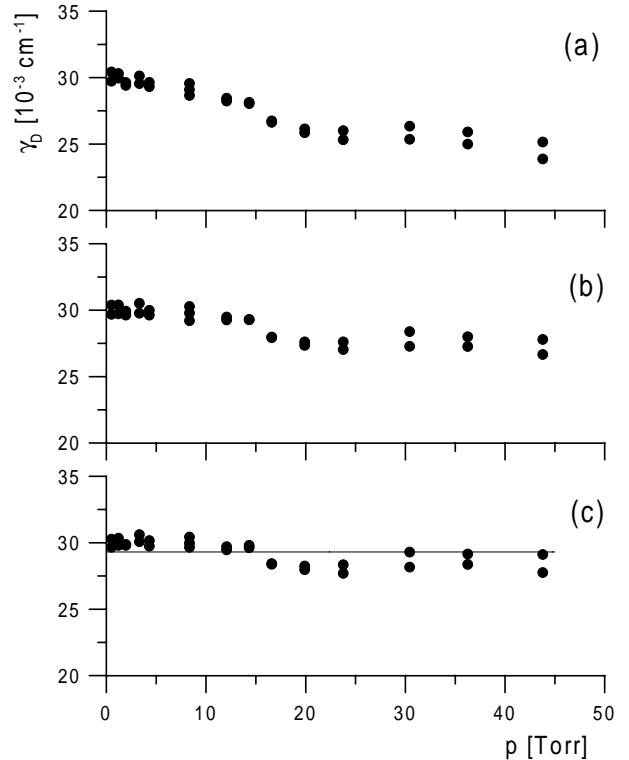


**Fig. 4.** Plots of the Doppler width  $\gamma_D$  (FWHM) of the 687.1 nm Ar line against the neon pressure  $p$  determined for different fitting profiles: (a)  $O_{VP}(\tilde{\nu})$  profile, (b)  $O_{SDVP}(\tilde{\nu})$  profile calculated for van der Waals potential, (c)  $O_{SDVP}(\tilde{\nu})$  profile calculated for Lennard-Jones potential. The mean value of  $\gamma_D$  is marked by solid line (—).

The argon pressure in the Ar–Ne mixture was kept constant at 0.72 torr. The line profiles were first analysed in terms of the ordinary Voigt profile by fitting the measured interferograms to the FPI response function  $O_{VP}(\omega)$  given by equation (2). The values of Doppler width  $\gamma_D$  determined from such fits are shown in Figure 4a where they are plotted against the neon pressure. It is seen that – unlike to the Ar–He system – in the case of perturbation by Ne the Doppler width  $\gamma_D$  of the 687.1 nm line decreases with the increase of the neon pressure. The observed decrease of the Doppler width was found

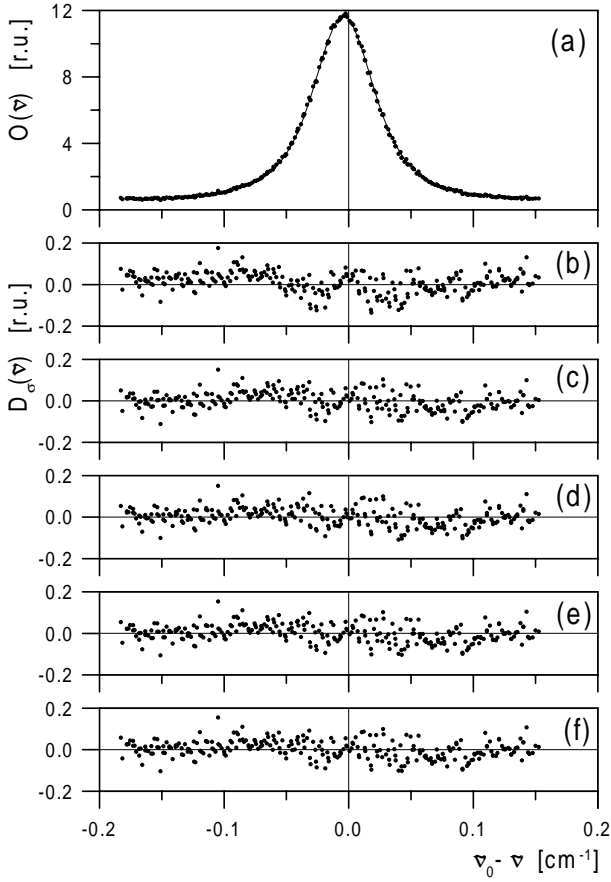


**Fig. 5.** (a) Shape of the 687.1 nm Ar line at neon pressure 36.26 torr, (•) experimental points, solid line (—) the best fit  $O_{VP}(\tilde{\nu})$  profile. (b) Weighted differences between the observed profile and the fitted  $O_{VP}(\tilde{\nu})$  profile with the constant  $\gamma_D$ . (c) Weighted differences between the observed profile and the fitted  $O_{VP}(\tilde{\nu})$  profile. (d) Weighted differences between the observed profile and the fitted  $O_{GP}(\tilde{\nu})$  profile with the constant  $\gamma_D$ . (e) Weighted differences between the observed profile and the fitted  $O_{SDVP}(\tilde{\nu})$  profile calculated for van der Waals potential. (f) Weighted differences between the observed profile and the fitted  $O_{SDVP}(\tilde{\nu})$  profile calculated for Lennard-Jones potential.

to be  $\Delta\gamma_D = (5.5 \pm 1.5) \times 10^{-3} \text{ cm}^{-1}$  for the neon pressure 43.79 torr.

Figure 5a shows an example of the measured profile of the 687.1 nm Ar line recorded at 36.26 torr of neon. The weighted differences  $D_\sigma(\omega)$  between the experimental and best fit values obtained from the Voigt analysis, equation (2), are plotted in Figures 5b and 5c. The weighted differences plotted in Figure 5b obtained assuming the constant Doppler width equal to  $29.5 \times 10^{-3} \text{ cm}^{-1}$  which corresponds to the gas temperature 320 K are a little bit worse than those plotted in Figure 5c obtained from the fit in which the Doppler width was varied.

The effect of narrowing of the Doppler component of the 687.1 nm Ar line perturbed by Ne which is clearly seen in Figure 4a must be regarded as an evidence that the line shape analysis based on the ordinary Voigt profile

fails in this case. The problem arises, however, whether the reduction of the Doppler width is caused by Dicke narrowing due to velocity-changing collisions or by speed-dependent effects giving rise to correlation between the Doppler and collisional broadening. It is also possible that the decrease of  $\gamma_D$  shown in Figure 4a may be caused by simultaneous occurrence of the Dicke narrowing and speed-dependent effect.

## 4 Dicke narrowing

In the neon pressure region for which measurements of the profiles of the 687.1 nm Ar line perturbed by Ne reported in the present work were performed, the mean free path between collisions may be of the same order of magnitude or less as the wavelength of the emitted radiation. This means that in this pressure region the velocity-changing collisions, and in particular the Dicke narrowing [3] may have noticeable influence on the observed line shapes. In order to verify whether such an influence really exists in our case we have performed numerical tests based on both the ordinary Galatry profile (GP) [4] and the speed-dependent Galatry profile (SDGP) [5] in which the Dicke narrowing is taken into account.

### 4.1 Fitting to the Galatry profile

Galatry [4] used so-called “soft-collision” model in which the emitter motion is treated as a diffusion motion and derived an expression for the profile of a collision-narrowed line hereafter referred to as the “ordinary” Galatry profile. The convolution of the Galatry profile and the instrumental function of FPI can be written in the following form

$$O_{GP}(\omega) = \frac{2}{\Omega} \left\{ \frac{1}{2} + \sum_{n=1}^{\infty} R^n e^{-nL} e^{-n^2 G^2/4} \times \exp \left[ -\frac{1}{2z^2} (zDn - 1 + e^{-zDn}) \right] \times \cos \left[ \frac{2n\pi}{\Omega} (\omega - \omega_0 - \Delta) \right] \right\}, \quad (3)$$

where following Herbert [30]

$$z = 2\sqrt{\ln 2} \frac{\nu}{\gamma_D} \quad (4)$$

is called the narrowing parameter, and  $\nu$  is the effective velocity-changing collision rate. Equation (3) represents a formula for the response of the FPI to the ordinary Galatry profile.

Unfortunately, neither theoretical nor experimental values of  $\nu$  are available in the literature so that the narrowing parameter  $z$  for the line under investigation is not known. Therefore an attempt was undertaken in the present work to determine  $z$  by fitting the profile  $O_{GP}(\omega)$ , equation (3), to our experimental profile of the 687.1 nm

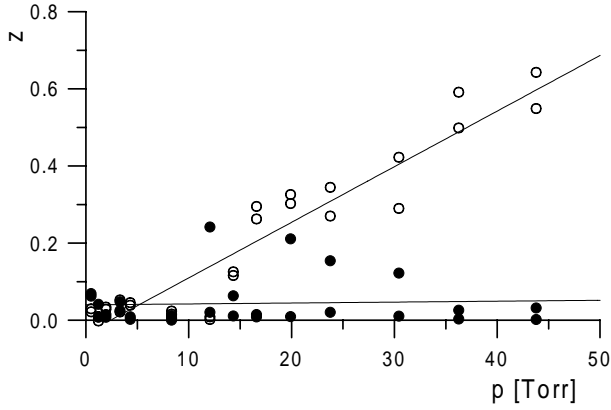


**Fig. 6.** Plots of the narrowing parameter  $z$  of the 687.1 nm Ar line against the neon pressure  $p$  determined on the basis of the  $O_{GP}(\tilde{\nu})$  ( $\circ$ ) and  $O_{SDGP}(\tilde{\nu})$  ( $\bullet$ ) profile. The fitted functions are plotted as solid lines (—).

Ar line perturbed by Ne. It was found that our experimental profiles can be well fitted to the Galatry profile with constant Doppler width  $\gamma_D = 29.5 \times 10^{-3} \text{ cm}^{-1}$  and the narrowing parameter  $z$  linearly dependent on the neon pressure. The values of the narrowing parameter  $z$  determined from such fits are shown in Figure 6 where they are plotted against the neon pressure. An example of the weighted differences between the experimental and best fit values obtained from the Galatry analysis, equation (3), are plotted in Figure 5d.

#### 4.2 Fitting to the speed-dependent Galatry profile

The response of the FPI to the speed-dependent Galatry profile [5] can be written in the form [24]

$$O_{SDGP}(\omega) = \frac{2}{\Omega} \left\{ \frac{1}{2} F_0(\omega) + \sum_{n=1}^{\infty} R^n \exp \left[ -\frac{G^2 n^2}{4} \right] F_n(\omega) \right\}, \quad (5)$$

where

$$F_n(\omega) = \exp \left[ -\frac{1}{4z^2} (2zDn - 3 + 4e^{-zDn} - e^{-2zDn}) \right] \times \frac{4}{\sqrt{\pi}} \int_0^{+\infty} dx x^2 e^{-x^2} \text{sinc} \left[ x \frac{1 - e^{-zDn}}{z} \right] \times \exp[-LB_W(x, \alpha)n] \times \cos \left[ \frac{2n\pi}{\Omega} (\omega - \omega_0 - \Delta B_S(x, \alpha)) \right]. \quad (6)$$

Here  $\text{sinc}(y) = \sin(y)/y$ . The functions  $B_W(x; \alpha)$  and  $B_S(x; \alpha)$  more precisely described in Section 5 are the reduced width and shift functions, respectively, which depend on the reduced emitter speed  $x = v_E/v_{m_E}$  and the mass ratio  $\alpha$ . Here  $v_E$  and  $v_{m_E} = \sqrt{2k_B T/m_E}$  are the emitter speed and its most probable speed, respectively.

Using the above expression for the SDGP we have repeated the same procedure which was used for the GP,

*i.e.* we have determined the  $z$ -values by fitting the profile  $O_{SDGP}(\omega)$ , equation (5), to our experimental profiles assuming that the emitter-perturber interaction can be described by the van der Waals potential. Again we have found that the speed-dependent Galatry profile can be fitted quite well to experimental profiles of the 678.1 nm Ar line but with  $z$ -values which differ from those determined in Section 4.1 from the fittings to the ordinary Galatry profile. The values of the narrowing parameter  $z$  determined from such fits are shown as black circles in Figure 6 where they are plotted against the neon pressure. In the present case the best fit of the profile  $O_{SDGP}(\omega)$  to experimental profiles was obtained for  $z$  close to zero for the whole region of neon pressures.

It is worthy to note that although the ordinary Galatry profile and speed-dependent Galatry profile functions are different the resulting profiles are numerically quite similar in the case of small collisional shift; both lead to good fits with experiment but with different values of  $z$ . The difference between  $z$ -values determined from fits based on the SDGP and those resulting from fits based on the ordinary GP reflects the essence of the difference between the physical content of the GP and SDGP functions. The small values of the narrowing parameter  $z$  obtained from the fit to the SDGP means that the narrowing of the Doppler component of the line is treated as caused by the correlation between the pressure and Doppler broadening. This means that the ordinary GP must be used with extreme caution since it can overestimate the role of the Dicke narrowing as was shown by Duggan *et al.* [15,18]. In the case when the GP is used the narrowing of the Doppler component of the line is interpreted as the result of the Dicke effect only. In such a case the influence of other narrowing effects, in particular those due to speed-dependent events, is completely ignored.

#### 4.3 Influence of the collisional narrowing on the shape of the 687.1 nm Ar line perturbed by Ne

If we neglect the correlations between velocity-changing and dephasing collisions described first by Rautian and Sobelman [7] we can evaluate the effective velocity-changing collision rate using a diffusion coefficient  $D$  for the emitter in the appropriate excited state in the perturbing gas. Such an effective velocity-changing collision rate is defined as  $\nu_{\text{diff}} = k_B T / (m_E D)$  where  $k_B$  is the Boltzmann constant. The diffusion coefficients for argon atoms excited to the states belonging to the configuration  $3p^5 4d$  in the buffer gas consisting of ground-state neon atoms are not known. Therefore the exact calculation of  $\nu_{\text{diff}}$  is not possible. We can assume that the interaction between excited Ar-atoms and ground state Ne-atoms can be described by a Lennard-Jones potential  $V(r) = C_{12}r^{-12} - C_6r^{-6}$ . Following Henry *et al.* [17] in such a case we can calculate  $D$  using expressions given by Hirschfelder *et al.* [31]. Then in the first approximation  $z_{\text{diff}} = 2\sqrt{\ln 2} \nu_{\text{diff}} / \gamma_D$

**Table 2.** The values force constants  $C_6$  and  $C_{12}$  used in line width and shift calculations for van der Waals potential  $V(r) = -C_6r^{-6}$  and Lennard-Jones potential  $V(r) = C_{12}r^{-12} - C_6r^{-6}$ .

System	State	$C_6$ [au]	$C_{12}$ [ $10^{10}$ au]
Ar*-He	upper	409	673
	lower	59	0.162
Ar*-Ne	upper	736	794
	lower	106	0.225

can be evaluated from the following expression:

$$z_{\text{diff}} = \frac{N\lambda\sigma^2\Omega^{(1,1)*}(T^*)}{\frac{3}{4}\sqrt{\pi}(1+m_E/m_P)}. \quad (7)$$

Here  $\lambda$  is a wavelength of the emitted radiation,  $\Omega^{(1,1)*}(T^*)$  is a dimensionless reduced integral [31] which is a function of a reduced temperature  $T^* = k_B T/\epsilon$ ,  $\sigma = (C_{12}/C_6)^{1/6}$  and  $\epsilon = C_6/(4C_{12})$  are the internuclear separation in which the interaction energy is equal to zero and the dissociation energy, respectively. In our estimates we have used the  $C_6$  and  $C_{12}$  values listed in Table 2. For the neon density  $13 \times 10^{17}$  atom  $\text{cm}^{-3}$  corresponding to a neon pressure of about 43 torr at temperature 320 K, we obtained  $z_{\text{diff}} \approx 1$ . It should be noted that results of recent studies by Pine [19,32], Duggan *et al.* [18], Lance *et al.* [33] and Joubert *et al.* [34] indicate that in some cases the correlations between velocity-changing and dephasing collisions of the type described by Rautian and Sobelman [7] may substantially affect the line profiles. If velocity-changing and dephasing collisions are partially correlated the parameter  $\nu$  occurring in the GP and SDGP [7,18] should be calculated from following relation  $\nu = \nu_{\text{diff}} - \eta(i\Delta + \gamma_L/2)$  where the correlation parameter  $\eta$  is defined as  $\eta = \nu_{\text{diff}}/\nu_T$  with  $\nu_T$  being the total collision rate. The parameter  $\eta$  can be varied between 0 and 1 for the uncorrelated and fully correlated case, respectively. For molecular lines of HF perturbed by Ar, Pine [19] determined  $\eta$  to be between 0.1 and 0.4 for different lines using hard-collision approach. If we assume  $z_{\text{diff}} = 1.0$  and  $\eta = 0.7$  as well as  $\gamma_D = 30 \times 10^{-3} \text{ cm}^{-1}$ ,  $\gamma_L = 50 \times 10^{-3} \text{ cm}^{-1}$ , and  $\Delta = 0$  we obtain in our case  $z \approx 0.03$ .

Moreover, the recent calculation performed by Leo *et al.* [35] shows that the Lennard-Jones potential can be much more repulsive than potentials calculated by other methods. Taking this into account we should emphasize that the above estimated value  $z_{\text{diff}} \approx 1$  is probably ten or more times greater than real values of this parameter.

We can now introduce the narrowing coefficient  $z/N$ . As was shown in the above discussion, the estimated value of the narrowing coefficient  $z/N$  can be between  $0.8 \times 10^{-18}/\text{atom cm}^{-3}$  and zero depending on the role of correlation between velocity-changing and dephasing collisions and on the unknown real  $\nu_{\text{diff}}$  value. On the other hand, the values of the narrowing coefficient  $z/N$  obtained using  $z$ -values plotted in Figure 6 evaluated by

means of the GP and SDGP are equal to  $(0.48 \pm 0.04) \times 10^{-18}/\text{atom cm}^{-3}$  and  $(0.01 \pm 0.03) \times 10^{-18}/\text{atom cm}^{-3}$ , respectively. This comparison shows that the  $z/N$ -value obtained from the line shape analysis strongly depends on the assumption made on the fitted profile. In our case the fitted value of the  $z$ -parameter is strongly dependent on the role which is played by speed-dependent effects. This is in agreement with results obtained by Duggan *et al.* [18] and Priem *et al.* [20].

According to equation (7) the narrowing coefficient  $z/N$  can be expressed by means the coefficient  $\nu/p$  which is frequently used in experimental work on Dicke narrowing. In our case the value  $\nu/p$  obtained from the ordinary GP analysis is equal to  $(0.19 \pm 0.02) \text{ cm}^{-1}/\text{atm}$ . This value is much higher than values obtained for some molecular lines [8,10,17,19], which were found to be smaller than  $0.1 \text{ cm}^{-1}/\text{atm}$ . Moreover, the assumption that collisional width and shift are speed-independent which is necessary to derive the GP is not justified in our case. This means that the value  $z/N = (0.01 \pm 0.03) \times 10^{-18}/\text{atom cm}^{-3}$  obtained by means of SDGP seems to be more reliable than that obtained from the analysis based on the GP. As a consequence, the Dicke narrowing seems to be too small to be registered in our experiment.

Therefore in the following section the Dicke narrowing will be neglected and profiles of the 687.1 nm line perturbed by Ne will be analysed taking into account only the speed-dependent effects which lead to the correlation between thermal motion and collisional broadening and shift of the line.

## 5 Speed-dependent effects

In order to check whether the statistical correlation between the thermal motion of emitter and its collision with a perturber can be responsible for the narrowing of the Doppler component of the 687.1 nm Ar line with the increase of the neon pressure we performed another line shape analysis based on the SDVP [1,2]. Now our experimental profiles were fitted to the profile  $O_{\text{SDVP}}(\omega)$  defined as a convolution of the SDVP and the instrumental function of the real FPI. Assuming the instrumental function of the FPI to have the form of convolution of an Airy function and the Gaussian profile, the profile  $O_{\text{SDVP}}(\omega)$  can be presented in the form analogous to equation (5) [24]

$$O_{\text{SDVP}}(\omega) = \frac{2}{\Omega} \left\{ \frac{1}{2} F_0(\omega) + \sum_{n=1}^{\infty} R^n \exp \left[ -\frac{G^2 n^2}{4} \right] F_n(\omega) \right\}, \quad (8)$$

where now

$$F_n(\omega) = \frac{4}{\sqrt{\pi}} \int_0^{+\infty} dx x^2 e^{-x^2} \text{sinc}[xDn] \times \exp[-LB_W(x, \alpha)n] \times \cos \left[ \frac{2n\pi}{\Omega} (\omega - \omega_0 - \Delta B_S(x, \alpha)) \right]. \quad (9)$$

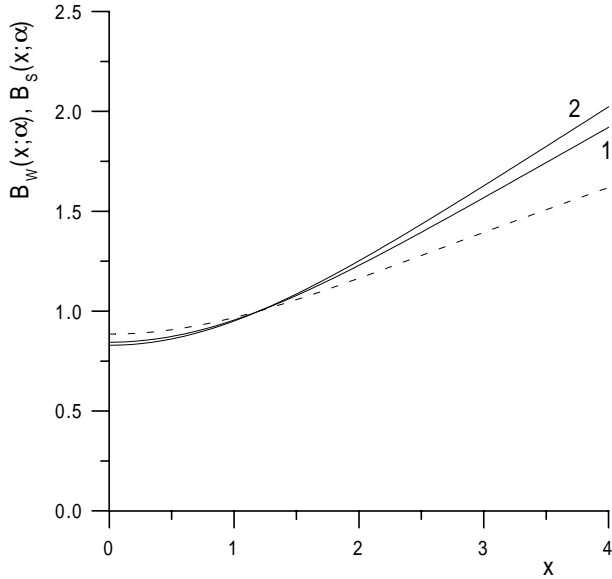


**Fig. 7.** Plots of  $B_W(x; \alpha)$  and  $B_S(x; \alpha)$  against  $x$  for the 687.1 nm Ar line perturbed by Ne ( $\alpha = 0.5$ ). Dashed line (---): for van der Waals potential ( $B_W(x; \alpha) \equiv B_S(x; \alpha)$ ). Solid line (—): for Lennard-Jones potential; curve 1:  $B_W(x; \alpha)$ , curve 2:  $B_S(x; \alpha)$ .

The profile  $O_{SDVP}(\omega)$  can be reduced to an expression derived in reference [36] and used in [37] for  $G = 0$ .

The reduced broadening and shift functions  $B_W(x; \alpha)$  and  $B_S(x; \alpha)$  were first introduced by Ward *et al.* [2], who have shown that for an inverse power potential  $V(r) = -C_q r^{-q}$  the following relation holds

$$B_W(x; \alpha) = B_S(x; \alpha) = (1 + \alpha)^{-(q-3)/(2q-2)} M\left(-\frac{q-3}{2q-2}, \frac{3}{2}, -\alpha x^2\right), \quad (10)$$

where  $M(a, b, z)$  is the confluent hypergeometric function. In general case of potentials of arbitrary form,  $B_W(x; \alpha)$  and  $B_S(x; \alpha)$  cannot be expressed in a closed form and the numerical calculations of expressions derived in reference [2] are required which can be done using formulas given in [36]. In the present work we first used the van der Waals potential which corresponds to  $q = 6$  in equation (10) and for which  $B_W(x; \alpha) = B_S(x; \alpha)$ . The plot of  $B_W(x; \alpha)$  on  $x$  calculated from equation (10) with  $q = 6$  and  $\alpha = 0.5$  for Ar\*-Ne system is shown in Figure 7 as a dashed line. We have also used the Lennard-Jones potential with the  $C_6$  and  $C_{12}$  constants listed in Table 2. The  $B_W(x; \alpha)$  and  $B_S(x; \alpha)$  functions calculated in this way are plotted against  $x$  in Figure 7 where they are shown as solid lines. It is seen that they differ markedly each other and from the functions corresponding to the van der Waals potential.

In Figures 4b and 4c the Doppler widths  $\gamma_D$  determined by the fits of our experimental profiles to the convolution  $O_{SDVP}(\omega)$  of the SDVP with the instrumental function of the FPI, equation (8) are plotted against the

neon pressure. It is seen that for the Lennard-Jones potential, Figure 4c, we find an apparent reduction of the narrowing of the Doppler component of the 687.1 nm Ar line perturbed by Ne, amounting to almost 100% at highest neon pressures. The mean value of the Doppler width is found to be  $(29.30 \pm 0.87) \times 10^{-3} \text{ cm}^{-1}$  which corresponds to the Doppler temperature  $(317 \pm 19) \text{ K}$  *i.e.* a value close to the gas temperature 320 K. As seen from Figure 4b the use of the van der Waals potential also gives rise to some reduction of the decrease of the Doppler width with increase of neon pressure, but we are unable to obtain 100% reduction. In this case we still obtain a decrease of the Doppler width below  $29.3 \times 10^{-3} \text{ cm}^{-1}$  which corresponds to  $z \approx 0.1$ . The use of the SDGP with van der Waals potential does not lead to the reduction of this decrease.

The weighted differences obtained from the SDVP analysis, equation (8), for the van der Waals and Lennard-Jones potentials are plotted in Figures 5e and 5f, respectively. It is true that the weighted differences shown in Figures 5c–5f look very similar. This means that there is no difference in the quality of the fits in the case of ordinary Voigt, Galatry and speed-dependent Voigt profile analysis of our measured interferograms. This is in accordance with results of numerical tests which show that the Voigt profile can be fitted to SDVP much better when collisional shift is negligible. To detect any differences in the quality of the fits the value of the signal to noise ratio should be much higher than that corresponding to our experimental set-up. Figure 5 also shows that the measured line shape is symmetrical. This is in agreement with experimental [15,18] and theoretical [2,9] results which show that the line shape asymmetry caused by the speed-dependent effects should not be expected when the collisional shift of the line can be neglected.

It should be emphasized that the neglect of correlation effects would lead to some errors in data analysis. Duggan *et al.* [15,18] showed that the neglect of speed-dependent effects can cause the value of the Dicke narrowing may to appear to be too large. In our case the Doppler width  $\gamma_D$  obtained from the ordinary Voigt analysis of the 687.1 nm Ar line at neon pressure 43.79 torr corresponds to Doppler temperature 222 K while the temperature determined by means of a thermocouple was found to be 320 K. Such a decrease of the Doppler width does not occur if the analysis based on the SDVP is done. Thus the neglect of correlation effects may be the cause of significant experimental errors as large as 30% in the determination of temperature. Thus one can conclude that correlation effects may be important also for systems when the emitter is heavier than the perturber as in the Ar\*-Ne case ( $\alpha = 0.5$ ).

The values of the Lorentzian width  $\gamma_L$  and shift  $\Delta$  determined by the fits of our experimental profiles to the profile  $O_{VP}(\omega)$ , equation (2), are shown in Figure 8 where they are plotted against the number density  $N$  of neon. We can see that both the width and shift are linear functions of  $N$ . It is interesting to note that contrary to the Doppler widths  $\gamma_D$ , the values of the Lorentzian widths  $\gamma_L$  and shifts  $\Delta$  determined on basis of the profile  $O_{SDVP}(\omega)$ ,



**Table 3.** Comparison of experimental values of the  $\beta$  and  $\delta$  coefficients (in units  $10^{-20}$  cm<sup>-1</sup>/atom cm<sup>-3</sup>) of the 687.1 nm argon line perturbed by neon with those calculated for different interatomic potentials. For experimental data the values of standard deviations are given.

Experimental	$\beta$	$\delta$	$\delta/\beta$
VP	$3.622 \pm 0.018$	$0.053 \pm 0.021$	$0.015 \pm 0.006$
SDVP-vdW	$3.583 \pm 0.018$	$0.054 \pm 0.022$	$0.015 \pm 0.006$
SDVP-LJ	$3.565 \pm 0.018$	$0.057 \pm 0.022$	$0.016 \pm 0.006$
Wawrzyński and Wolnikowski [21]	$4.12 \pm 0.33$ ( $3.81 \pm 0.31$ )	$0.30 \pm 0.14$ ( $0.28 \pm 0.13$ )	$0.07 \pm 0.04$
Theoretical	$\beta$	$\delta$	$\delta/\beta$
vdW	2.737	-0.995	-0.363
LJ	6.421	0.801	0.125

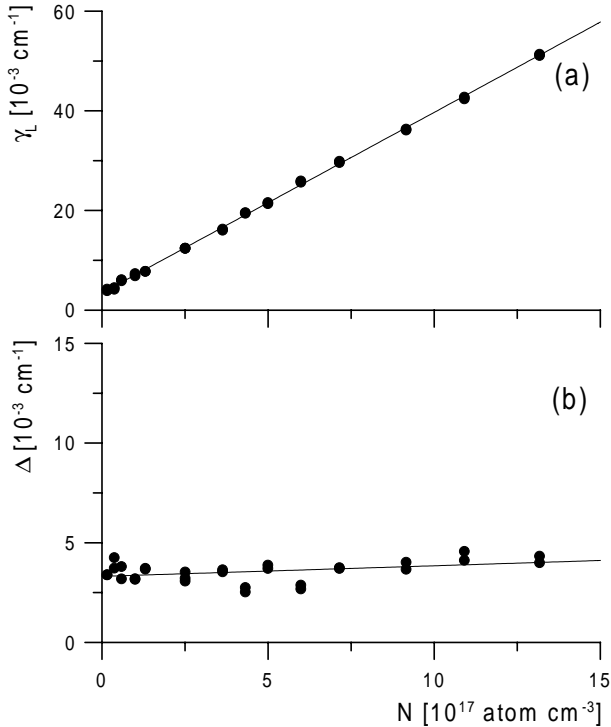


**Fig. 8.** Plots of (a) the Lorentzian width (FWHM)  $\gamma_L$  and (b) shift  $\Delta$  for the 687.1 nm Ar line against the neon density  $N$  determined on the basis of the  $O_{VP}(\tilde{\nu})$  profile. The fitted functions are plotted as solid lines (—).

equation (8), do not differ significantly from those determined on the basis of the traditional Voigt analysis, equation (2).

It should be noted that in general case the correlation effects may lead to a nonlinear density dependence of the Lorentzian width and shift and also to an asymmetry of the profile. Nevertheless, as it is seen from Figure 8 our Lorentzian width and shift are linearly dependent on the density. Similar behaviour was reported by Lewis and his co-workers [11] who performed a very careful analysis of the influence of the correlation effects on the Ca 422.7 nm line perturbed by rare gases.

The fact that we have not observed any asymmetry of the profiles is in accordance with the prediction of the theory due to Ward *et al.* [2], who have shown that no asymmetry is expected when the shift  $\Delta$  is vanishingly small. As it is seen from Figure 8b and Table 3 the shift coefficients determined in the present work are close to zero.

Using the plots of the Lorentzian widths  $\gamma_L$  and shifts  $\Delta$  against the neon density, the values of the pressure broadening  $\beta$  and shift  $\delta$  coefficients were determined from the slopes of straight lines plotted in Figure 8. These experimental coefficients are listed in Table 3, where the values determined from the fits of experimental profiles to the profile  $O_{VP}(\omega)$ , equation (2), are denoted by “VP”. The values denoted by “SDVP-vdW” and “SDVP-LJ” are the coefficients determined on the basis of the speed-dependent analysis with the profile  $O_{SDVP}(\omega)$ , equation (8), with van der Waals and Lennard-Jones potentials, respectively. Table 3 also contains the experimental values determined by Wawrzyński and Wolnikowski [21] who, however, as in the Ar–He case did not include the Gaussian contribution to their FPI instrumental function. The values of  $\beta$  and  $\delta$  given in parentheses in Table 3 are the experimental values of reference [21] recalculated for the gas temperature 320 K. It is seen from Table 3 that the experimental values of the pressure broadening ( $\beta$ ) and ( $\delta$ ) coefficients obtained by the speed-dependent Voigt profile analysis are only slightly different (less than 2% of  $\beta$  value) than those obtained by the ordinary Voigt procedure. A similar behaviour was found by the Lewis group in their studies on the Ca 422.7 nm line perturbed by rare gases [11].

It should be noted that the experimental values of the pressure shift coefficient  $\delta$  for the 687.1 nm Ar line perturbed by Ne are close to zero. This corroborates the conclusion expressed by Ward *et al.* [2] that correlation effects do not produce any asymmetry of the line shape when the pressure shift is very small.

Our experimental  $\beta$  and  $\delta$  values for Ar–Ne differ from those reported by Wawrzyński and Wolnikowski [21]. It should be noted, however, that their measurements were performed for much lower densities of perturbing gas and the precision of their experimental arrangement

was almost one order of magnitude smaller than in the present work.

## 6 Discussion

The problem of accurate theoretical interpretation of the pressure broadening ( $\beta$ ) and shift ( $\delta$ ) coefficient of the 687.1 nm Ar line is not easy to solve at the present time. This line arises due to transition between the  $3p^5(2P_{3/2}^o)4d[1/2]_1^o$  and  $3p^5(2P_{3/2}^o)4p[1/2]_1$  states in the Racah notation. Both the upper  $3p^54d$  and lower  $3p^54p$  configurations form several levels and the coupling between levels within a given configuration has to be taken into account in calculations of the Lorentzian width  $\gamma_L$  and shift  $\Delta$  [38,39]. If the coupling between levels is ignored then we can estimate the values  $\gamma_L$  and  $\Delta$  using a purely adiabatic impact theory in the form given by Lindholm and Foley [40,41]. To make an attempt at a crude interpretation of our broadening and shift coefficients we have performed calculation based on the van der Waals (vdW) and Lennard-Jones (LJ) potentials. The values of  $\beta$  and  $\delta$  obtained from these calculations are listed in Tables 1 and 3 for Ar\*-He and Ar\*-Ne systems, respectively. The force constants  $C_6$  and  $C_{12}$  used in these calculations [24] were obtained using Unsöld approximation [42] and an expression given by Hindmarsh *et al.* [43]. They are listed in Table 2. Data necessary to evaluate force constants were taken from [44–46].

As it is seen theoretical values of  $\beta$  and  $\delta$  obtained from the adiabatic Lindholm-Foley theory are in poor agreement with our experimental data. It should be emphasized, however, that results of calculation based on a purely adiabatic approach such as that due to Lindholm and Foley must be regarded as the estimates only and, as stressed by Peach [39] they “may give results in error by a factor of two or more”. A proper description of the broadening and shift coefficients requires a semi-classical non-adiabatic approach or better a fully quantum treatment in which close-coupled equations are solved using the methods of scattering theory. Such semi-classical non-adiabatic and quantum close-coupled calculations were performed by Leo *et al.* [35,47] for some self-broadened helium and neon lines. For argon lines no calculations of this type have been performed up to now. We hope that the experimental results presented here will motivate future theoretical investigation of the broadening and shift of the argon lines.

The main goal of this work is to present results of experimental investigations which show that the Doppler width of the 687.1 nm Ar line perturbed by Ne determined using a Voigt-type analysis decreases with the neon pressure and to try to interpret such a behaviour. The observed narrowing of the Doppler component of the profile cannot be treated as marginal effect since – as was found – the Doppler temperature determined by means of a Voigt profile is almost 100 K lower than the gas temperature.

The accurate interpretation of our results is difficult because the signal-to-noise ratio in our experiment is still too low to observe systematic differences between measured interferograms and fitted profiles. In such a case the

analysis of the fit quality is not useful because all used profiles give the same quality of the fit. Similar behaviour was recently reported by Priem *et al.* [20] in their study of profiles of CO lines perturbed by N<sub>2</sub> and O<sub>2</sub>. They found that both the SDVP and ordinary GP can be fitted very well to collisionally unshifted CO lines; the quality of the fits is the same for both the SDVP and GP.

The discussion presented in the present work shows that the observed narrowing of the Doppler component of the line can be interpreted as a manifestation of the correlation between the collisional and Doppler broadening. We have also discussed the Dicke narrowing as a phenomenon which can lead to the same effect. Nevertheless in our opinion the observed narrowing of the Doppler component of the 687.1 nm Ar line perturbed by Ne is caused rather by speed-dependent effects. Unfortunately, the final conclusion cannot be formulated at the present time due to the lack of the accurate data on the diffusion coefficient for the Ar\*-Ne system and the real potentials describing the interaction between the Ar-atom excited to states belonging to the  $3p^54d$  and  $3p^54p$  configurations and the ground-state Ne-atom.

In general case, the reduction of the Doppler width with perturber gas pressure may be due to simultaneous occurrence of the Dicke narrowing and Doppler-collision correlations and it is possible that a part of observed narrowing can be caused by the Dicke narrowing. However, in order to investigate the Dicke narrowing in the case when speed-dependent effects occur, the close-coupled calculations of pressure broadening and shift coefficients based on realistic interatomic potentials must first be performed. Recently, such an analysis was done by Pine [19] for HF lines perturbed by Ar for which strong collisional shift occurs.

We wish to thank Dr. Pine for making accessible reference [19] before its publication. We also wish to thank Dr. Rohart for making accessible reference [20] before its publication. We are grateful to the referees for their helpful comments and critical remarks. This work was supported by a grant No. 673/P03/96/10 (2 P03B 005 10) from the State Committee for Scientific Research.

## References

1. P.R. Berman, J. Quant. Spectrosc. Radiat. Transf. **12**, 1331 (1972).
2. J. Ward, J. Cooper, E.W. Smith, J. Quant. Spectrosc. Radiat. Transf. **14**, 555 (1974).
3. R.H. Dicke, Phys. Rev. **89**, 472 (1953); J.P. Wittke, R.H. Dicke, Phys. Rev. **103**, 620 (1956).
4. L. Galatry, Phys. Rev. **122**, 1218 (1961).
5. R. Ciuryło, J. Szudy, J. Quant. Spectrosc. Radiat. Transf. **57**, 411 (1997).
6. M. Nelkin, A. Ghatak, Phys. Rev. **135**, A4 (1964).
7. S.G. Rautian, I.I. Sobelman, Usp. Fiz. Nauk **90**, 209 (1966) [Sov. Phys. Usp. **9**, 701 (1967)].
8. B. Lance, G. Blanquet, J. Walrand, J.P. Bouanich, J. Mol. Spectrosc. **185**, 262 (1997).

9. R. Ciurylo, Phys. Rev. A **58**, 1029 (1998).
10. B. Lance, D. Robert, J. Chem. Phys. **109**, 8283 (1998).
11. E.L. Lewis, *Spectral Line Shapes*, edited by J. Szudy (Ossolineum Publ., Wrocław, 1988), Vol. 5, p. 485; M. Harris, E.L. Lewis, D. McHugh, I. Shannon, J. Phys. B **17**, L661 (1984); J. Phys. B **19**, 3207 (1986); I. Shannon, M. Harris, D. McHugh, E.L. Lewis, J. Phys. B **19**, 1409 (1986).
12. R.L. Farrow, L.A. Rahn, G.O. Sitz, G.J. Rosasco, Phys. Rev. Lett. **63**, 746 (1989).
13. D. Robert, J.M. Thuet, J. Bonamy, S. Temkin, Phys. Rev. A **47**, R771 (1993).
14. F. Rohart, H. Mäder, H.W. Nicolaisen J. Chem. Phys. **101**, 6475 (1994); F. Rohart, A. Ellendt, F. Kaghat, H. Mäder, J. Mol. Spectrosc. **185**, 222 (1997).
15. P. Duggan, P.M. Sinclair, A.D. May, J.R. Drummond, Phys. Rev. A **51**, 218 (1995).
16. P.M. Sinclair, J.Ph. Berger, X. Michaut, R. Saint-Loup, R. Chaux, H. Berger, J. Bonamy, D. Robert, Phys. Rev. A **54**, 402 (1996).
17. A. Henry, D. Hurtmans, M. Margottin-Maclou, A. Valentin, J. Quant. Spectrosc. Radiat. Transf. **56**, 647 (1996); note a missprint in equation (A1):  $\hbar$  should be replaced by  $\pi$ .
18. P. Duggan, P.M. Sinclair, R. Berman, A.D. May, J.R. Drummond, J. Mol. Spectrosc. **186**, 90 (1997).
19. A.S. Pine, J. Quant. Spectrosc. Radiat. Transf. **62**, 397 (1999).
20. D. Priem, F. Rohart, J.M. Colmont, G. Włodarczak, J.P. Bouanich, J. Mol. Structure (in press).
21. J. Wawrzyński, J. Wolnikowski, Phys. Scripta **33**, 113 (1986).
22. R. Ciurylo, A. Bielski, J. Domyslawska, J. Szudy, R.S. Trawiński, J. Phys. B **27**, 4181 (1994).
23. A. Bielski, J. Wolnikowski, Acta Phys. Pol. A **54**, 601 (1978).
24. R. Ciurylo, Ph.D. thesis, Nicholas Copernicus University, Toruń, 1998.
25. A. Bielski, W. Dokurno, E. Lisicki, Z. Turło, Opt. Appl. **9**, 151 (1981).
26. A.G. Jiglinskii, V.V. Kuchinskii, *Real Fabry-Perot interferometer* (Mashinostroyeniye, Leningrad, 1983).
27. D.W. Marquardt, J. Soc. Industr. Appl. Math. **11**, 431 (1963).
28. A. Bielski, S. Brym, R. Ciurylo, J. Domyslawska, E. Lisicki, R.S. Trawiński, J. Phys. B **27**, 5863 (1994).
29. E.A. Ballik, App. Opt. **5**, 170 (1966).
30. F. Herbert, J. Quant. Spectrosc. Radiat. Transf. **14**, 943 (1974).
31. J.O. Hirschfelder, C.F. Curtiss, R.B. Bird, *Molecular Theory of Gases and Liquids* (Wiley, New York, 1954).
32. A.S. Pine, J. Chem. Phys. **101**, 3444 (1994).
33. B. Lance, S. Ponsar, J. Walrand, M. Lepere, G. Blanquet, J.P. Bouanich, J. Mol. Spectrosc. **189**, 124 (1998).
34. P. Joubert, J. Bonamy, D. Robert, J.L. Domenech, D. Bermejo, J. Quant. Spectrosc. Radiat. Transf. **61**, 519 (1999).
35. P.J. Leo, D.F.T. Mullanphy, G. Peach, V. Venturi, I.B. Whittingham, J. Phys. B **30**, 535 (1997).
36. R. Ciurylo, A. Bielski, S. Brym, J. Jurkowski, J. Quant. Spectrosc. Radiat. Transf. **53**, 493 (1995).
37. S. Brym, R. Ciurylo, R.S. Trawiński, A. Bielski, Phys. Rev. A **56**, 4501 (1997).
38. G. Peach, Adv. Phys. **30**, 367 (1981).
39. G. Peach, in *Atomic, Molecular and Optical Physics Handbook*, edited by G.W.F. Drake (AIP Press, Woodbury, NY, 1998), p. 669.
40. E. Lindholm, Arkiv. Mat. Astr. Fys. **28B**, No. 3 (1941).
41. H.M. Foley, Phys. Rev. **69**, 616 (1946).
42. A. Unsöld, *Physik der Sternatmosphären* (Springer, Berlin, 1955).
43. W.R. Hindmarsh, A.D. Petford, G. Smith, Proc. Roy. Soc. A **247**, 296 (1967).
44. C.E. Moore, *Atomic Energy Levels* (Nati. Bur. Stand. (U.S.) Circ. **467**, 1960).
45. J. Stiehler, J. Hinze, J. Phys. B **28**, 4055 (1995).
46. A. Bielski, J. Wasilewski, Z. Naturforsch. **35a**, 1112 (1980).
47. P.J. Leo, D.F.T. Mullanphy, G. Peach, I.B. Whittingham, J. Phys. B **25**, 1161 (1992); J. Phys. B **28**, 4449 (1995); P.J. Leo, G. Peach, I.B. Whittingham, J. Phys. B **28**, 591 (1995); P.J. Leo, D.F.T. Mullanphy, G. Peach, V. Venturi, I.B. Whittingham, J. Phys. B **29**, 4573 (1996); Acta Phys. Pol. A **98**, 459 (1998).